Title
Ultrathin Durable Organic Hydrophobic Coatings Enhancing Dropwise Condensation Heat Transfer.

Journal
Langmuir: the ACS journal of surfaces and colloids, 38(37)

Authors
Tripathy, Abinash
Regulagadda, Kartik
Lam, Cheuk
et al.

Publication Date
2022-09-20

DOI
10.1021/acs.langmuir.2c01477

Peer reviewed

LANGMUIR

pubs.acs.org/Langmuir Article

Ultrathin Durable Organic Hydrophobic Coatings Enhancing Dropwise Condensation Heat Transfer

Abinash Tripathy,[⊥] Kartik Regulagadda,[⊥] Cheuk Wing Edmond Lam, Matteo A. Donati, Athanasios Milionis, Chander Shekhar Sharma, Efstratios Mitridis, Thomas M. Schutzius, and Dimos Poulikakos*

Cite This: *Langmuir* 2022, 38, 11296–11303 Read Online

ACCESS | Metrics & More | Article Recommendations | Supporting Information

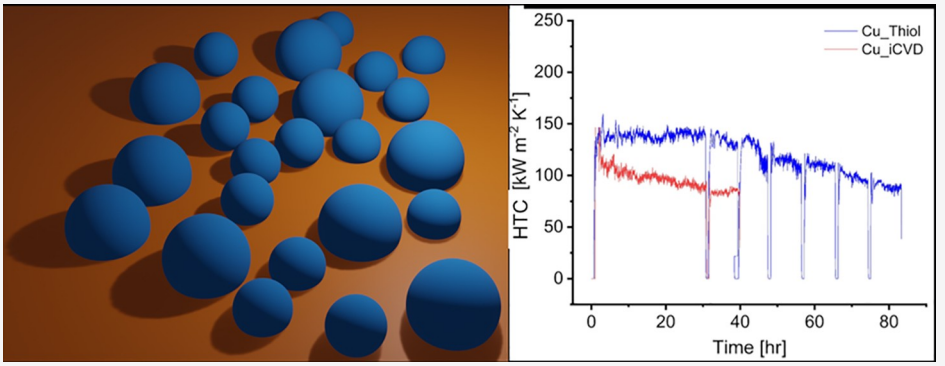

ABSTRACT: Organic hydrophobic layers targeting sustained dropwise condensation are highly desirable but suffer from poor chemical and mechanical stability, combined with low thermal conductivity. The requirement of such layers to remain ultrathin to minimize their inherent thermal resistance competes against durability considerations. Here, we investigate the long-term durability and enhanced heat-transfer performance of perfluorodecanethiol (PFDT) coatings compared to alternative organic coatings, namely, perfluorodecyltriethoxysilane (PFDTS) and perfluorodecyl acrylate (PFDA), the latter fabricated with initiated chemical vapor deposition (iCVD), in condensation heat transfer and under the challenging operating conditions of intense flow (up to 9 m s^{-1}) of superheated steam (111 °C) at high pressures (1.42 bar). We find that the thiol coating clearly outperforms the silane coating in terms of both heat transfer and durability. In addition, despite being only a monolayer, it clearly also outperforms the iCVD-fabricated PFDA coating in terms of durability. Remarkably, the thiol layer exhibited dropwise condensation for at least 63 h (>2× times more than the PFDA coating, which survived for 30 h), without any visible deterioration, showcasing its hydrolytic stability. The cost of thiol functionalization per area was also the lowest as compared to all of the other surface hydrophobic treatments used in this study, thus making it the most efficient option for practical applications on copper substrates.

INTRODUCTION

Condensation of water vapor plays a vital role in multiple energy conversion applications such as thermal management, power generation, refrigeration, air conditioning, and water desalination.[1−4] Depending on the formation and growth of the condensate on the surface, condensation can be distinguished into two different modes, i.e., filmwise condensation (FWC) and dropwise condensation (DWC). Due to its, up to by an order of magnitude, higher heat-transfer coefficient, DWC is highly desired in all heat-transfer applications.[5−9] Most of the condenser surfaces (copper, aluminum, steel, etc.) used in the industry are naturally hydrophilic. Hence, to achieve DWC on such surfaces, an additional hydrophobic coating is required.[10−17] However, the long-term durability of such coatings is a major bottleneck for practical applications. Typically, durability can be enhanced by increasing the coating thickness. Since organic coatings have low thermal conductivity (e.g., 0.3 W m^{-1} K^{-1} for Teflon),[18,19] increasing the thickness will increase thermal resistance and thus reduce the heat-transfer performance, an undesired counterproductive outcome. An ideal hydrophobic coating should simultaneously achieve high droplet shedding efficiency, low thermal resistance, high mechanical durability, and low-cost scalable fabrication capability. It is obviously a great challenge to develop a coating exhibiting all of these properties.

Received: June 8, 2022
Revised: August 17, 2022
Accepted: August 17, 2022
Published: August 29, 2022

https://doi.org/10.1021/acs.langmuir.2c01477
Langmuir 2022, 38, 11296−11303

Recent works studied the durability of polymer coatings using initiated chemical vapor deposition (iCVD)[5,20] and chemical vapor deposition (CVD)[21] in condensation environments. The advantage of these techniques is that they can produce ultrathin (tens of nanometers) and conformal hydrophobic coatings, which are expected to be considerably more robust compared to monolayers. However, such coatings have not been exposed for a prolonged time in a harsh condensing environment (high-temperature shear flow), while their durability has only been compared with one type of hydrophobic monolayer, i.e., a silane coating.[5] Comparing iCVD-fabricated coating with existing monolayers is very critical to understanding the true potential of this technique because the iCVD technique lacks in terms of scalability compared to silanization or thiolation and needs special adaptation for practical applications, which can be expensive.[5,22,23] Towards this, we investigate the heat-transfer performance and durability of a 1H,1H,2H,2H-perfluorodecanethiol (PFDT) coating and compare it with those of 1H,1H,2H,2H-perfluorodecyltriethoxysilane (PFDTS) and 1H,1H,2H,2H-perfluorodecyl acrylate (PFDA) coatings, the latter fabricated using iCVD, on flat copper substrates. The thiol coating outperformed the silane coating in terms of both durability and enhancement in heat transfer, and unexpectedly outperformed the PFDA coating using iCVD in terms of durability. Furthermore, the thiol coating is found to be the most economical hydrophobic surface treatment costing ~2.5 times less than the grafted PFDA polymer coating using iCVD.

RESULTS AND DISCUSSION

Fabrication of Hydrophobic Surfaces. We have fabricated three different surfaces with silane (PFDTS), thiol (PFDT), and grafted polymer (PFDA), the latter using the iCVD technique on flat copper substrates (RMS roughness of flat uncoated copper surface used = 22 nm, see Methods). Further, as a reference for FWC, we used a copper oxide (CuO) nanostructured surface without any organic coating[8,9] (for details of fabrication, see Methods, Figure S1) and a clean flat copper surface. Figure S2a shows a scanning electron microscopy image of the reference surface. We adopted a sessile drop method to measure surface wettability. The reference CuO nanostructured surface showed superhydrophilic behavior with a static contact angle (SCA) of ~0° (see Figure S2b). For the clean flat copper surface, the advancing contact angle (ACA) was 38.3 ± 5.6°, and contact angle hysteresis (CAH) was 23.6 ± 5.3°. Both silane and thiol involve a simple dip coating step (see Methods). The static contact angle, advancing contact angle, and contact angle hysteresis were measured for all of the fabricated surfaces. Both silane-coated (SCA, 114.4 ± 0.9°; ACA, 123.3 ± 0.6°; CAH, 21.3 ± 1.2°) and thiol-coated (SCA, 113.6 ± 1.1°; ACA, 134 ± 2.7°; CAH, 27 ± 2.2°) substrates exhibited hydrophobic behavior. The grafted polymer coating using iCVD was deposited in two steps (see Methods, Figure 1a). In this process, we adopt a solvent-free approach to deposit in the gaseous phase an ultrathin film and graft it to the substrate to enhance durability.[22,24] Film deposition using iCVD is conformal, and the thickness of the coating can be precisely controlled. After some thickness optimization tests, an ultrathin layer (~40 nm) of PFDA was deposited on a flat copper substrate, leading to a hydrophobic coating (SCA, 119.6 ± 1.1°; ACA, 127 ± 3°; CAH, 10.3 ± 3.4°). In Figure 1b, we have plotted the advancing contact angle and contact

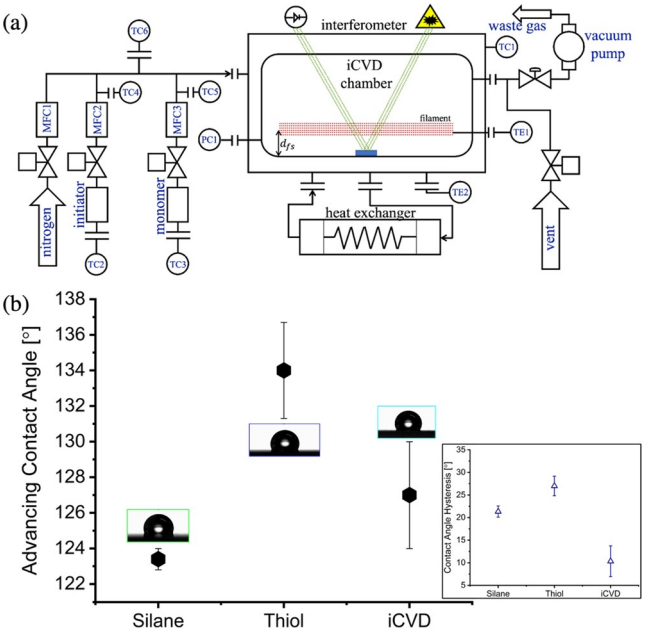

Figure 1. (a) Schematic of the iCVD tool used to deposit the PFDA polymer coating on copper substrates. (b) Advancing contact angle and contact angle hysteresis (inset) of water droplets on hydrophobic copper substrates.

angle hysteresis (inset) of water droplets for all of the hydrophobic (silane, thiol, and PFDA using iCVD) copper substrates. A lower CAH implies that dropwise condensation is enhanced, leading to a higher heat-transfer coefficient (HTC). However, CAH is not the only parameter influencing the HTC; nucleation site density and population distribution do affect HTC.[25−28] Therefore, it is challenging to predict the outcome of condensation purely on the basis of CAH.

Microscale Condensation Behavior. Since most of the heat transfer during DWC is attributed to droplets with diameters <100 μm,[29−31] we characterized the microscale condensation behavior of water droplets on all of the hydrophobic test substrates using environmental scanning electron microscopy (ESEM, see Methods, and Video S1). Figure 2 shows the selected snapshots captured at similar droplet diameters on all of the test substrates. For silane-, thiol-, and PFDA-coated surfaces, the contact angles of the growing condensed droplets varied between 40 and 120°,[32] and we observed distinct droplets showcasing their ability to manifest DWC. If we compare this result with the macroscopic contact angles, we can conclude that all three surfaces show good hydrophobic performance. Apparently, on the short term and without being challenged, all coatings appear to be good candidates for enhancing the condensation heat transfer.

Heat-Transfer Measurement at High Pressures. We evaluated the performance of all of the test substrates under harsh conditions in a high-pressure flow chamber (pressure, P = 1.42 bar) by exposing them to superheated steam at temperature, T = 111 ± 0.3 °C. The flow direction of the superheated steam was vertically downward (in the direction of gravity, see Figure S3a). The samples were tested at two steam velocities, i.e., V = 3 m s^{-1} (laminar flow, $Re = \frac{\rho VD}{\mu} = 1300$, where ρ = steam density = 0.82 kg-m^{-3}, V = steam velocity, D = hydraulic diameter, and μ = dynamic viscosity of steam = 12.62 μPa-s)[8], and V = 9 m s^{-1} (transition flow, Re = 3900).

https://doi.org/10.1021/acs.langmuir.2c01477
Langmuir 2022, 38, 11296−11303

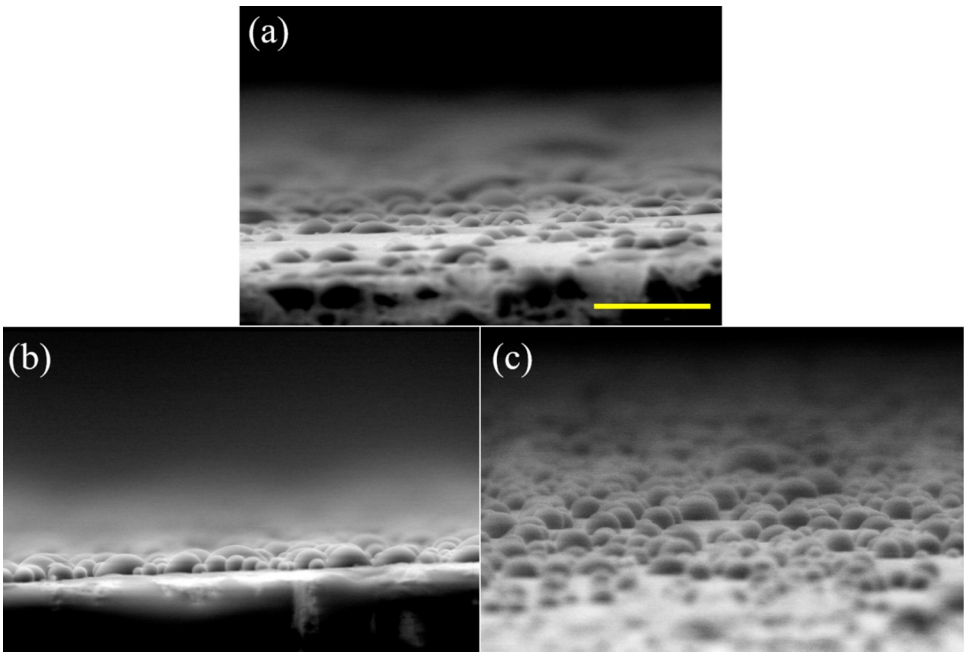

Figure 2. Water condensation on test substrates observed using ESEM: (a) silane-coated copper, (b) thiol-coated copper, and (c) PFDA-coated copper using iCVD (scale bar, 100 μm; all images have the same magnification).

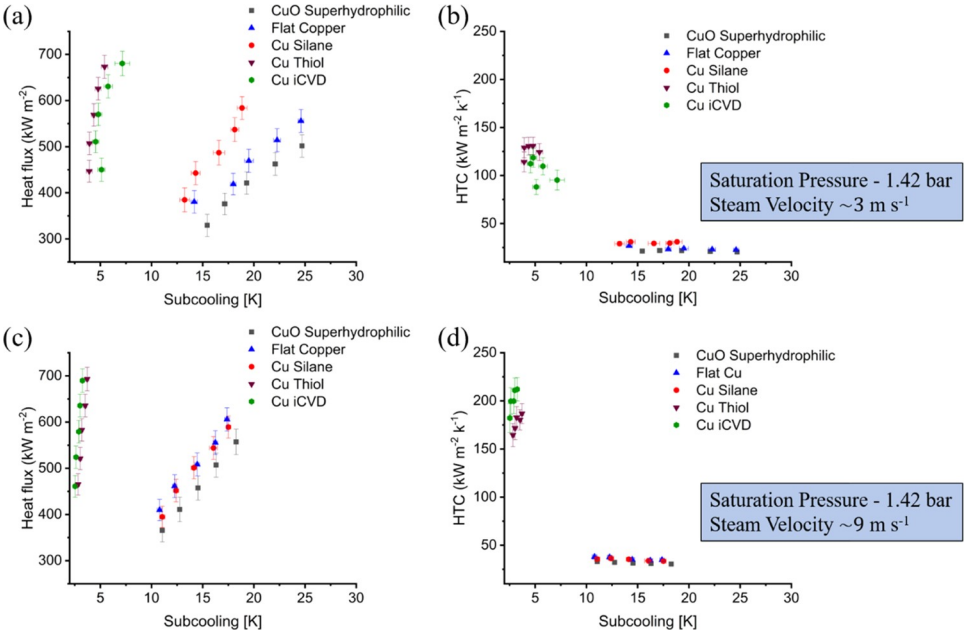

Figure 3. Heat flux (a), (c) and heat-transfer coefficient (HTC) (b), (d) for all of the substrates vs. subcooling at steam velocities of 3 m s^{-1} (a and b) and 9 m s^{-1} (c and d) and steam saturation pressure of 1.42 bar.

This setup (see Figure S3b) enables us to study the effect of vapor shear on the hydrophobic coating present on the surface during condensation.

Figure 3 shows the heat flux and heat-transfer coefficient (HTC) data for all of the test substrates with respect to subcooling, $\Delta T = T - T_s$, where T is the steam temperature and T_s is the surface temperature of the substrate. The silane-coated copper substrate failed right at the beginning of the experiment; as soon as the steam flow started, we observed FWC on the surface with a significant decrease in HTC. Further, the subcooling on the silane-coated copper substrate was slightly lower than that on the reference CuO nanostructured surface and the clean flat copper surface. This might be due to the presence of mixed DWC and FWC on the silane-coated copper substrate. However, it was difficult to optically confirm this during the experiment due to initial fogging on the viewing window, which prevented capturing a clear snapshot with the camera. Both the thiol-coated and PFDA-coated copper substrates exhibited DWC in the flow chamber until the end of the experiment (~3 to 4 h). For V = 3 and 9 m s^{-1}, the thiol-coated copper substrate showed enhancements of ~6 and ~5.8 times in HTC, respectively, as compared to the reference substrates (CuO nanostructured surface and the cleaned flat copper surface) for FWC. Similarly, the PFDA-

https://doi.org/10.1021/acs.langmuir.2c01477
Langmuir 2022, 38, 11296−11303

coated copper substrate also manifested DWC with ~5.1 and ~6.6 times enhancements in HTC at V = 3 and 9 m s^{-1}, respectively. In our experiments, both vapor shear and gravity play a role in the droplet slide-off events since both act in the same direction during condensation. Considering the experimental error limits, both thiol and PFDA coatings using iCVD exhibited similar heat-transfer performance. The silane-coated copper, CuO nanostructured surface, and the clean flat copper surface exhibited FWC with similar values of HTC. For DWC, the total thermal resistance between the substrate and steam is lower compared to FWC.[8,12] This causes the T_s value to be closer to the steam temperature T in the case of DWC. For this reason, we have a narrow range of ΔT for thiol- and iCVD-coated copper substrates (which exhibited DWC) and the range of ΔT is larger for the CuO nanostructured, clean flat copper- and silane-coated copper substrates (which exhibited FWC). We also calculated the average droplet departure diameter of the water droplets on the PFDA coating using iCVD and thiol coating. For the PFDA coating using iCVD, the average droplet departure diameter (d_{avg}) values were 2 ± 0.4 mm and 1.5 ± 0.2 for steam velocities V = 3 and 9 m s^{-1}, respectively. Similarly, for the thiol coating, the d_{avg} values were found to be 2.4 ± 0.4 and 1.8 ± 0.2 mm for steam velocities V = 3 and 9 m s^{-1}, respectively.

In contrast to low-pressure conditions typically used in condensers, here, much harsher conditions (high pressures and temperatures) were used as an accelerated aging test, providing an indication for the prolonged performance of the substrates.[8,33] The steam conditions in our test chamber are designed to challenge the coatings in different ways. Compared to conditions in condensers found in typical steam cycles, i.e., saturated steam at pressures on the order of tens of millibars and approximately room temperature, the pressure and temperature in our chamber are much higher. In addition, steam flow in a narrow channel, where our test surfaces are installed, exposes them to high shear stresses. For a steam flow of 3 m s^{-1} in our chamber, the maximum shear stress on the coating from the steam flow is estimated to be at least 65 mPa, from our recent work.[8] As dropwise condensation proceeds, repeated droplet departure exposes the bare coating (as the condensate is removed) to these stresses by which it is worn over time until eventual failure. The coating lifespan we provide here serves as a starting reference for estimation of the actual lifespan, as these shear stresses vary in industrial conditions depending on specific operational requirements and condenser designs, resulting in different steam flow profiles. Therefore, this experiment confirms that both thiol- and PFDA-coated copper substrates using iCVD can well withstand such harsh conditions with an enhancement in HTC. To further test the robustness of these two coatings, we also performed longer durability tests (discussed next) in the flow chamber until the substrates failed, i.e., the mode of condensation transitioned from DWC to FWC.

Durability Test. For the durability tests on the thiol- and PFDA-coated copper substrates, we maintained the same chamber conditions for a prolonged time, i.e., P = 1.42 bar, T = 111 ± 0.3 °C, and V = 3 m s^{-1}. The test was run initially for 30 h continuously on a given substrate. Then, we shut down the steam flow (leaving the substrate inside the flow chamber) and restarted the test the next day, running it for 8 h before shutting down the steam flow again. This 8 h cycle was repeated every day until the substrate fails. During the tests, we used high-speed imaging to observe the temporal variation of the condensation events on the substrates (see Figure 4a,b). Surprisingly, despite the thiol thickness being at the molecular

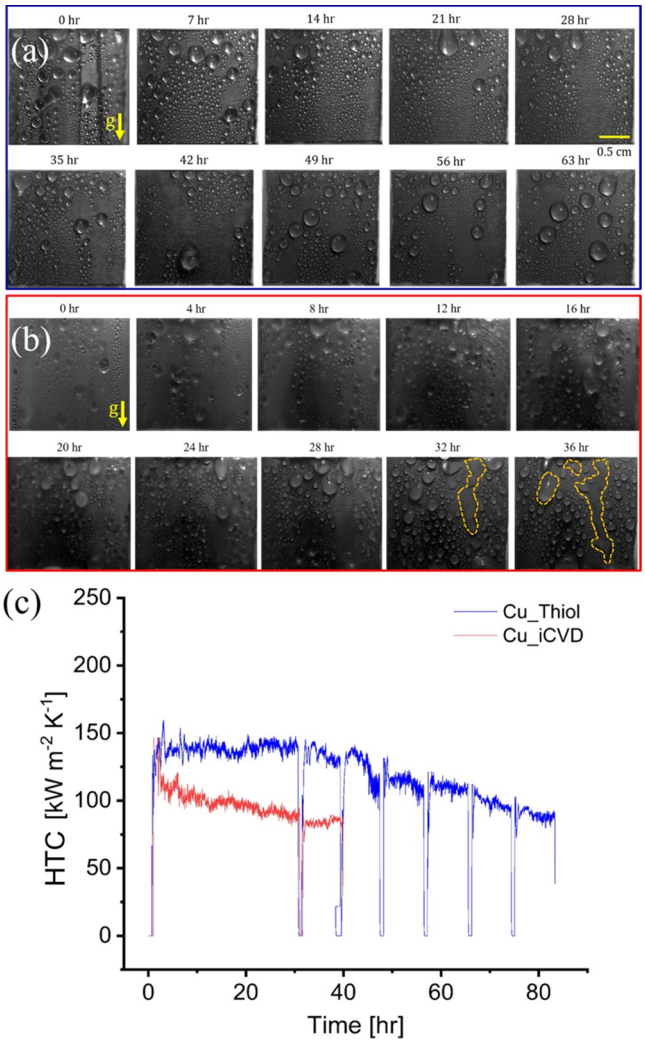

Figure 4. Temporal evolution of condensation on (a) thiolated and (b) PFDA-coated copper surfaces. The regions with the orange dashed line show the localized FWC on the PFDA-coated surface. (c) Heat-transfer coefficient (HTC) plotted vs. time during the durability experiment to observe the trend. Whenever we shut down the steam flow at the end of the experiment, there is an obvious decrease in HTC between shutdown and restart.

level (monolayer)[34] compared to the ~40 nm thickness of the iCVD coating, the former exhibited DWC for about 63 h, whereas the PFDA-coated copper substrate could sustain DWC for about 30 h. The images in Figure 4b corresponding to 32 and 36 h of steam exposure, respectively, clearly show localized FWC on the PFDA-coated copper substrate as depicted by the dashed line. Further, the thiol-coated copper substrate maintained higher HTC (Figure 4c) throughout the test and survived without any visual degradation of its DWC for up to 63 h.

Regarding the wettability of both substrates, ACA and CAH were measured after the durability test (see Table S1). The increase in CAH proves that the coatings indeed failed eventually, leading to localized FWC. The higher degree of robustness of thiol as compared to that of the PFDA coating can be explained in terms of the bonds it forms with the

https://doi.org/10.1021/acs.langmuir.2c01477
Langmuir 2022, 38, 11296−11303

substrate. Prior to PFDA coating, we treat the copper surface with a trichlorovinylsilane (TCVS) layer (see Methods). This provides anchoring points for the PFDA coating using its vinyl groups ($-CH_2$).[20] The vinyl group in TCVS forms a strong bond with the vinyl group in PFDA. On the other hand, silane is known to form oxane (Si−O) bonds with the surface hydroxyl groups present on the substrate. However, the surface oxide on copper is not hydrolytically stable. We believe that the oxide dissolves when exposed to water[35,36] and the bond between silane and copper breaks. In the case of the PFDA coating, even a small defect in the PFDA coating can cause the underlying surface to be exposed to water, which would cause the failure of TCVS and hence PFDA coating.

In contrast, thiol directly forms a very strong covalent bond ($M + HS-(CH_2)_n-R \rightarrow MS-(CH_2)_n-R$, M—Metal, $HS-(CH_2)_n-R$—general formula of thiol where H is hydrogen and S is sulfur)[37,38] with the copper substrate and therefore is hydrolytically more stable than silane. Thus, the higher degree of robustness of thiol as compared to that of the PFDA coating can be explained in terms of the bonds it forms with the substrate. Our result is in contrast with the literature where the grafted PFDA polymer using iCVD on aluminum has been claimed to be the most robust for water condensation compared with silane.[5] In the same work, the authors demonstrated a successful prototype of iCVD coating on a copper substrate exhibiting DWC. As thiol does not bind well with aluminum, we have used a copper substrate in this study. Thus, a simple thiol coating can be really promising for practical applications on copper substrates. In this work, the superiority of thiol coating over PFDA coating using iCVD has been demonstrated specifically for superheated steam under extreme temperature (111 ± 0.3 °C) and flow speed ($3\ m\ s^{-1}$) at high pressure (1.42 bar).

Further, thiol can be coated on any metal used for a condenser, with an additional copper layer using electroplating,[39,40] physical vapor deposition,[41,42] etc. Since copper has very high thermal conductivity ($401\ W\ m^{-1}\ K^{-1}$),[8] such an additional layer should hardly affect the overall heat-transfer efficiency.

Cost Calculation. We then calculated the costs of all of the hydrophobic coatings studied. The cost estimation includes the cost of cleaning the surfaces, electricity used to operate the tools used in the process, and the cost of all of the chemicals used. The costs of silane, thiol, and PFDA coatings for an area of 1 m^2 in US dollars (USD) are 320, 304, and 771, respectively (see Supplementary Information, Section S2). Additionally, the equipment purchase cost required for the iCVD tool (~USD 216250) is much higher than that of the minimal equipment that the thiol functionalization requires. Therefore, thiol could be used for practical applications for long-term DWC considering its robustness, easy and scalable coating process, and low cost.

CONCLUSIONS

We have demonstrated the long-term durability of thiol coating as compared to silane and PFDA polymer-grafted coatings using iCVD. Silane-coated copper substrates immediately failed in the flow condensation setup as soon as the steam flow is initiated. At 3 and 9 $m\ s^{-1}$ steam velocity, the thiol-coated copper substrate exhibited enhancements of 6 and 5.8 times in HTC, respectively, compared to the reference CuO nanostructured superhydrophilic substrate. The PFDA-coated copper sample also showed similar heat-transfer performance. In the durability test, however, the thiol-coated copper substrate maintained DWC for about 63 h, whereas the PFDA polymer-grafted copper surface exhibited localized FWC already after 30 h. Further, the thiol-coated substrate proved to be more economical with a cost estimation per area 2.5 times less than that of the PFDA polymer grafting. Considering their superior durability, cost-effectiveness, and competitive heat-transfer performance, thiol treatment can be an efficient strategy for industrial applications related to condensation heat transfer.

EXPERIMENTAL METHODS

Fabrication. Copper substrate (EN CW004A, Metall Service Menziken Inc., Switzerland, 20 mm × 50 mm and 3 mm thick) was first sonicated in acetone, IPA, and DI water (10 min each) followed by drying in nitrogen (N_2). Then, the substrates were functionalized by different hydrophobic treatments.

For preparing the CuO nanostructured reference substrate (see Figure S1), an alkali solution was prepared by mixing sodium chlorite ($NaClO_2$), sodium hydroxide (NaOH), and sodium phosphate tribasic dodecahydrate ($Na_3PO_4{\cdot}2H_2O$) in DI water.[9,15] The solution was vigorously stirred using a magnetic stirring bead. Then, the solution was heated to 95 °C, and the substrate was dipped in the hot alkali solution for 4 min until the surface turns black. The substrate was then rinsed with DI water and dried in N_2 blow.

Hydrophobic Treatments. *Silane.* Clean flat copper substrates were dipped in a solution containing 1H,1H,2H,2H-perfluorodecyltriethoxysilane in hexane for 2 h followed by drying on a hotplate at 120 °C for 45 min.

Thiol. Clean flat copper substrates were immersed in a solution of 1 mM 1H,1H,2H,2H-perfluorodecanethiol (Sigma-Aldrich) in ethanol for 1 h. Then, the substrates were rinsed three times with ethanol and dried with N_2.

Hydrophobic Polymer Coating Using iCVD. Grafted polymer coating using iCVD was performed in two steps.[19,21] First, we coated the flat copper substrate with trichlorovinylsilane (TCVS, Sigma-Aldrich) in a custom-made chemical vapor deposition chamber at ~80 mTorr. Post-TCVS coating, we utilized the iCVD tool (iLab Coating System, GVD Corporation) to deposit an ultrathin layer of 1H,1H,2H,2H-perfluorodecyl acrylate (PFDA; 97%, with tert-butylcatechol as an inhibitor, Sigma-Aldrich) as a monomer in the presence of tert-butyl peroxide (TBPO; 98%, Sigma-Aldrich) as an initiator. The chamber pressure was kept at ~100 mTorr, the temperature of the chamber base was kept at 39 °C, and the filament temperature for the decomposition of the monomer and initiator was kept at 300 °C. The coating time was 15 min.

Surface Characterization. The surface morphology of the CuO nanostructured substrate was captured with a Hitachi SU8230 scanning electron microscope (see Figure S2a). We performed the static contact angle and contact angle hysteresis measurement for the water droplets on each test sample using a DataPhysics OCA 35 goniometer. All of the images of the droplets during the measurements were captured using an in-built camera, and the contact angle and contact angle hysteresis values were obtained using ImageJ software.[43] The thickness measurement of the iCVD-coated polymer film was performed using a Woollam VASE ellipsometer (incidence angles −65, 70, and 75°; wavelength −400 to 800 nm; Cauchy-Urbach model fit).[44] The roughness of the cleaned flat copper surface before coating was measured by an atomic force microscope (AFM, Oxford Instruments MFP 3D origin PPP-NCH-20).

Environmental Scanning Electron Microscopy (ESEM). Contact angles of the growing condensed droplets were observed on the substrates during condensation of pure water vapor and its subsequent evaporation with environmental scanning electron microscopy (ESEM) (Quanta 650 FEG, FEI). First, the sample was attached vertically onto a custom-designed mount using a silver paste, such that the viewing angle would be almost parallel to the surface. The mount with the sample attached was then placed onto the

https://doi.org/10.1021/acs.langmuir.2c01477
Langmuir 2022, 38, 11296−11303

cooling stage of the ESEM instrument. The temperature of the stage was controlled by a thermistor, a Peltier device, and a recirculating chiller. After that, the chamber was pumped and purged multiple times with water vapor. Under vacuum, the beam was turned on at a voltage of 20 kV and a spot size of 3.0 but temporarily blanked to protect the surface.[45,46] Then, the chamber pressure was set to 500 Pa and the cooling stage was set to 2 °C. To initiate condensation, a target pressure of 775 Pa with a ramping rate of 100 Pa min^{-1} was set. As the pressure increased and reached 625 Pa, the beam was activated, and image acquisition was started. Condensation commenced and progressed on the surface, with image contrast and brightness of the image occasionally adjusted to compensate for the effects from the condensate droplets. After some time, the chamber pressure was reduced to a target of 500 Pa at a ramping rate of 100 Pa min^{-1} for imaging evaporation. Finally, the beam was blanked, and image acquisition was stopped. The pressure adjustment procedure was repeated to observe condensation and evaporation at several locations of the sample. We performed at least three cycles of condensation for each substrate.

Experimental Procedure for Condensation Experiments at High Pressures. We performed the flow condensation experiments in a custom-built chamber, as shown in Figure S3a. The test substrates were exposed to a steam temperature, T = 111 °C and a pressure, P = 1.42 bar.[8] The steam velocity, V, was maintained at 3 and 9 m s^{-1}. In all our experiments, the sample size was 2 cm × 2 cm. A high-speed imaging camera was used to capture the condensation dynamics on the surfaces. The imaging was somewhat hindered at the beginning of each experiment (0 h) due to fogging on the viewing glass caused by the condensed droplets. A stable water layer was then formed on the viewing glass after ∼2 h, reducing the fogging effect and providing the necessary transparency to capture the condensation dynamics on the sample surface clearly. We used a copper block (cooled by recirculating chiller 1, Figure S3a) with a series of thermocouples at the back of the sample to measure the heat flux, and the heat-transfer coefficient was calculated by estimating the surface temperature using a separate thermocouple (see Figure S3a,b). We ensured one-dimensional heat conduction along the thermocouple array by providing air insulation at the sides of the copper block. The noncondensed steam coming from the test substrate was allowed to enter a secondary condenser where the steam was cooled by a secondary chiller (chiller 2, Figure S3b) and condensed back to liquid water. This liquid water flows under gravity back to the boiler, thus completing the condensation loop. To measure the steam temperature and surface temperature of the substrate (Figure S3a), we used two separate thermocouples to get the subcooling ($\Delta T = T - T_s$, where T is the steam temperature and T_s is the surface temperature of the substrate) values during the experiment. At the beginning of each experiment, we used a vacuum pump to evacuate the chamber to a pressure below 20 mbar to reduce noncondensable gases, followed by pumping deionized water from the reservoir into the chamber until a pressure of 1.7 bar. During this process, the residual gases (remaining noncondensable gases) rise to the top of the test chamber (Figure S3a), and we use a valve to remove them. This process was repeated until all residual gases were removed from the condensation loop. We always maintained the chamber pressure higher than the atmospheric pressure to avoid the ingress of atmospheric air. Steam is generated by heating the boiler and lowering the pressure in the condensation loop during the experiments. We changed the temperature of the coolant in chiller 1 to achieve different subcooling values. The heat flux along the condensing test substrate was estimated as $q'' = -K\frac{\Delta T}{\Delta x}$, where q'' is the heat flux, K is the thermal conductivity of copper, and $\frac{\Delta T}{\Delta x}$ is the slope of the measured temperature vs axial distance plot in the copper block. Finally, the HTC was calculated as $h = q''/\Delta T$. We followed the exact same procedure as described in our previous work by Donati and Lam *et al.*[8] For the durability test, the steam velocity, V, was maintained at 3 m s^{-1}. The durability tests were performed as described in the main text.

■ ASSOCIATED CONTENT

Supporting Information

The Supporting Information is available free of charge at https://pubs.acs.org/doi/10.1021/acs.langmuir.2c01477.

CuO nanostructured surface fabrication process, SEM image of the CuO nanostructured surface, wettability of the CuO nanostructured surface, schematic of the flow condensation setup at high pressures, wettability data before and after the durability experiment, and cost estimation of hydrophobic coatings (PDF)

Video of microcondensation behavior of water on all hydrophobic test substrates (Video S1) (MP4)

Video of condensation behavior on silane-, thiol-, and PFDA-coated copper surfaces (Video S2, replayed 33X slower) (MP4)

Durability experiment of thiol- and PFDA-coated copper surfaces (Video S3, replayed 33X slower) (MP4)

■ AUTHOR INFORMATION

Corresponding Author

Dimos Poulikakos − *Laboratory of Thermodynamics in Emerging Technologies, Department of Mechanical and Process Engineering, ETH Zurich, CH-8092 Zurich, Switzerland;* orcid.org/0000-0001-5733-6478; Email: dpoulikakos@ethz.ch; Fax: +41 44 632 11 76

Authors

Abinash Tripathy − *Laboratory of Thermodynamics in Emerging Technologies, Department of Mechanical and Process Engineering, ETH Zurich, CH-8092 Zurich, Switzerland;* orcid.org/0000-0003-3546-2806

Kartik Regulagadda − *Laboratory of Thermodynamics in Emerging Technologies, Department of Mechanical and Process Engineering, ETH Zurich, CH-8092 Zurich, Switzerland*

Cheuk Wing Edmond Lam − *Laboratory of Thermodynamics in Emerging Technologies, Department of Mechanical and Process Engineering, ETH Zurich, CH-8092 Zurich, Switzerland;* orcid.org/0000-0002-8782-8438

Matteo A. Donati − *Laboratory of Thermodynamics in Emerging Technologies, Department of Mechanical and Process Engineering, ETH Zurich, CH-8092 Zurich, Switzerland;* orcid.org/0000-0003-0197-0159

Athanasios Milionis − *Laboratory of Thermodynamics in Emerging Technologies, Department of Mechanical and Process Engineering, ETH Zurich, CH-8092 Zurich, Switzerland;* orcid.org/0000-0002-0049-1255

Chander Shekhar Sharma − *Thermofluidics Research Lab, Department of Mechanical Engineering, Indian Institute of Technology Ropar, Rupnagar, Punjab 140 001, India;* orcid.org/0000-0002-6193-6457

Efstratios Mitridis − *Laboratory of Thermodynamics in Emerging Technologies, Department of Mechanical and Process Engineering, ETH Zurich, CH-8092 Zurich, Switzerland;* Present Address: Nanomaterials Engineering Research Group, Department of Chemistry and Applied Biosciences, Vladimir-Prelog-Weg 1, CH-8093 Zurich, Switzerland; orcid.org/0000-0002-0748-1471

Thomas M. Schutzius − *Laboratory of Thermodynamics in Emerging Technologies, Department of Mechanical and Process Engineering, ETH Zurich, CH-8092 Zurich, Switzerland;* Present Address: Laboratory for Multiphase

Thermofluidics and Surface Nanoengineering, Department of Mechanical and Process Engineering, ETH Zurich, Sonneggstrasse 3, CH-8092 Zurich, Switzerland; orcid.org/0000-0003-3309-3568

Complete contact information is available at: https://pubs.acs.org/10.1021/acs.langmuir.2c01477

Author Contributions

[⊥]A.T. and K.R. contributed equally to this work. A.T., A.M., C.S.S., and D.P. conceived the research. A.M., C.S.S., and D.P. provided scientific guidance throughout. A.T. fabricated and characterized all of the samples used in this study. A.T., K.R., and M.D. performed all of the condensation experiments in the flow condensation setup and analyzed the data. C.W.E.L. did the microcondensation observation on all surfaces using ESEM. E.M. and T.S. developed and optimized the protocol for iCVD coating. The manuscript was written with the help of all authors.

Funding

This project has received funding from the European Union's Horizon 2020 research and innovation program under grant number 801229 (HARMoNIC).

Notes

The authors declare no competing financial interest.

All of the data used in the main manuscript and the Supplementary Information to support the claims are available from the corresponding author upon reasonable request. The authors declare no competing financial interest.

■ ACKNOWLEDGMENTS

The authors thank Mr. Jovo Vidic for his help in the setup of the data acquisition system, Mr. Peter Feusi for his help in the construction of the condensation chamber for the heat-transfer experiments, Mr. Iwan Haechler for the AFM measurements, and the Cleanroom Operations Team of the Binnig and Rohrer Nanotechnology Center (BRNC) for their help and support.

■ REFERENCES

(1) Attinger, D.; Frankiewicz, C.; Betz, A. R.; Schutzius, T. M.; Ganguly, R.; Das, A.; Kim, C.-J.; Megaridis, C. M. Surface Engineering for Phase Change Heat Transfer: A Review. *MRS Energy Sustainable* **2014**, *1*, 1−40.

(2) Enright, R.; Miljkovic, N.; Alvarado, J. L.; Kim, K.; Rose, J. W. Dropwise Condensation on Micro-and Nanostructured Surfaces. *Nanoscale Microscale Thermophys. Eng.* **2014**, *18*, 223−250.

(3) Cho, H. J.; Preston, D. J.; Zhu, Y.; Wang, E. N. Nanoengineered Materials for Liquid-Vapour Phase-Change Heat Transfer. *Nat. Rev. Mater.* **2017**, *2*, 1−17.

(4) Edalatpour, M.; Liu, L.; Jacobi, A. M.; Eid, K. F.; Sommers, A. D. Managing Water on Heat Transfer Surfaces: A Critical Review of Techniques to Modify Surface Wettability for Applications with Condensation or Evaporation. *Appl. Energy* **2018**, *222*, 967−992.

(5) Paxson, A. T.; Yagüe, J. L.; Gleason, K. K.; Varanasi, K. K. Stable Dropwise Condensation for Enhancing Heat Transfer via the Initiated Chemical Vapor Deposition (iCVD) of Grafted Polymer Films. *Adv. Mater.* **2014**, *26*, 418−423.

(6) Rykaczewski, K.; Paxson, A. T.; Anand, S.; Chen, X.; Wang, Z.; Varanasi, K. K. Multimode Multidrop Serial Coalescence Effects during Condensation on Hierarchical Superhydrophobic Surfaces. *Langmuir* **2013**, *29*, 881−891.

(7) Mulroe, M. D.; Srijanto, B. R.; Ahmadi, S. F.; Collier, C. P.; Boreyko, J. B. Tuning Superhydrophobic Nanostructures to Enhance Jumping-Droplet Condensation. *ACS Nano* **2017**, *11*, 8499−8510.

(8) Donati, M.; Lam, C. W. E.; Milionis, A.; Sharma, C. S.; Tripathy, A.; Zendeli, A.; Poulikakos, D. Sprayable Thin and Robust Carbon Nanofiber Composite Coating for Extreme Jumping Dropwise Condensation Performance. *Adv. Mater. Interfaces* **2021**, *8*, No. 2001176.

(9) Tripathy, A.; Lam, C. W. E.; Davila, D.; Donati, M.; Milionis, A.; Sharma, C. S.; Poulikakos, D. Ultrathin Lubricant-Infused Vertical Graphene Nanoscaffolds for High-Performance Dropwise Condensation. *ACS Nano* **2021**, *15*, 14305−14315.

(10) Sharma, C. S.; Combe, J.; Giger, M.; Emmerich, T.; Poulikakos, D. Growth Rates and Spontaneous Navigation of Condensate Droplets Through Randomly Structured Textures. *ACS Nano* **2017**, *11*, 1673−1682.

(11) Sharma, C. S.; Lam, C. W. E.; Milionis, A.; Eghlidi, H.; Poulikakos, D. Self-Sustained Cascading Coalescence in Surface Condensation. *ACS Appl. Mater. Interfaces* **2019**, *11*, 27435−27442.

(12) Sharma, C. S.; Stamatopoulos, C.; Suter, R.; Von Rohr, P. R.; Poulikakos, D. Rationally 3D-Textured Copper Surfaces for Laplace Pressure Imbalance-Induced Enhancement in Dropwise Condensation. *ACS Appl. Mater. Interfaces* **2018**, *10*, 29127−29135.

(13) Mahapatra, P. S.; Ghosh, A.; Ganguly, R.; Megaridis, C. M. Key Design and Operating Parameters for Enhancing Dropwise Condensation through Wettability Patterning. *Int. J. Heat Mass Transf.* **2016**, *92*, 877−883.

(14) Ghosh, A.; Beaini, S.; Zhang, B. J.; Ganguly, R.; Megaridis, C. M. Enhancing Dropwise Condensation through Bioinspired Wettability Patterning. *Langmuir* **2014**, *30*, 13103−13115.

(15) Enright, R.; Miljkovic, N.; Dou, N.; Nam, Y.; Wang, E. N. Condensation on Superhydrophobic Copper Oxide Nanostructures. *J. Heat Transfer* **2013**, *135*, No. 091304.

(16) Miljkovic, N.; Enright, R.; Nam, Y.; Lopez, K.; Dou, N.; Sack, J.; Wang, E. N. Jumping-Droplet-Enhanced Condensation on Scalable Superhydrophobic Nanostructured Surfaces. *Nano Lett.* **2013**, *13*, 179−187.

(17) Miljkovic, N.; Enright, R.; Wang, E. N. Effect of Droplet Morphology on Growth Dynamics and Heat Transfer during Condensation on Superhydrophobic Nanostructured Surfaces. *ACS Nano* **2012**, *6*, 1776−1785.

(18) Price, D. M.; Jarratt, M. Thermal Conductivity of PTFE and PTFE Composites. *Thermochim. Acta* **2002**, *392*−*393*, 231−236.

(19) Cai, X.; Jiang, Z.; Zhang, X.; Gao, T.; Yue, K.; Zhang, X. Thermal Property Improvement of Polytetrafluoroethylene Nanocomposites with Graphene Nanoplatelets. *RSC Adv.* **2018**, *8*, 11367−11374.

(20) Khalil, K.; Soto, D.; Farnham, T.; Paxson, A.; Katmis, A. U.; Gleason, K.; Varanasi, K. K. Grafted Nanofilms Promote Dropwise Condensation of Low-Surface-Tension Fluids for High-Performance Heat Exchangers. *Joule* **2019**, *3*, 1377−1388.

(21) Miljkovic, N.; Preston, D. J.; Enright, R.; Wang, E. N. Electrostatic Charging of Jumping Droplets. *Nat. Commun.* **2013**, *4*, No. 2517.

(22) Alf, M. E.; Asatekin, A.; Barr, M. C.; Baxamusa, S. H.; Chelawat, H.; Ozaydin-Ince, G.; Petruczok, C. D.; Sreenivasan, R.; Tenhaeff, W. E.; Trujillo, N. J.; Vaddiraju, S.; Xu, J.; Gleason, K. K. Chemical Vapor Deposition of Conformal, Functional, and Responsive Polymer Films. *Adv. Mater.* **2009**, *22*, 1993−2027.

(23) Yagüe, J. L.; Gleason, K. K. Enhanced Cross-Linked Density by Annealing on Fluorinated Polymers Synthesized via Initiated Chemical Vapor Deposition To Prevent Surface Reconstruction. *Macromolecules* **2013**, *46*, 6548−6554.

(24) Gupta, M.; Gleason, K. K. Initiated Chemical Vapor Deposition of Poly(1H,1H,2H,2H-Perfluorodecyl Acrylate) Thin Films. *Langmuir* **2006**, *22*, 10047−10052.

(25) Sikarwar, B. S.; Khandekar, S.; Agrawal, S.; Kumar, S.; Muralidhar, K. Dropwise Condensation Studies on Multiple Scales. *Heat Transfer Eng.* **2012**, *33*, 301−341.

(26) Rose, J. W. Some Aspects of Condensation Heat Transfer Theory. *Int. Commun. Heat Mass Transf.* **1988**, *15*, 449−473.

(27) Hannemann, R. J.; Mikic, B. B. An Analysis of the Effect of Surface Thermal Conductivity on the Rate of Heat Transfer in Dropwise Condensation. *Int. J. Heat Mass Transf.* **1976**, *19*, 1299−1307.
(28) Carey, V. P. *Liquid-Vapor Phase-Change Phenomena*, 3rd ed.; CRC Press, 2020.
(29) Glicksman, L. R.; Hunt, A. W. Numerical Simulation of Dropwise Condensation. *Int. J. Heat Mass Transf.* **1972**, *15*, 2251−2269.
(30) Graham, C.; Griffith, P. Drop Size Distributions and Heat Transfer in Dropwise Condensation. *Int. J. Heat Mass Transf.* **1973**, *16*, 337−346.
(31) Kim, S.; Kim, K. J. Dropwise Condensation Modeling Suitable for Superhydrophobic Surfaces. *J. Heat Transfer* **2011**, *133*, No. 081502.
(32) Jung, Y. C.; Bhushan, B. Wetting Behaviour during Evaporation and Condensation of Water Microdroplets on Superhydrophobic Patterned Surfaces. *J. Microsc.* **2008**, *229*, 127−140.
(33) Torresin, D.; Tiwari, M. K.; Del Col, D.; Poulikakos, D. Flow Condensation on Copper-Based Nanotextured Superhydrophobic Surfaces. *Langmuir* **2013**, *29*, 840−848.
(34) Love, J. C.; Estroff, L. A.; Kriebel, J. K.; Nuzzo, R. G.; Whitesides, G. M. Self-Assembled Monolayers of Thiolates on Metals as a Form of Nanotechnology. *Chem. Rev.* **2005**, *105*, 1103−1170.
(35) Arkles, B. Silane Coupling Agents: Connecting Across Boundaries. *J. Organomet. Chem.* **2014**, *3*, 1−76.
(36) The Concept of Coupling with Organofunctional Silanes, Dow Corning, USA 2009. https://krayden.com/pdf/xia_silane_chemistry.pdf (accessed May 27, 2022).
(37) Reit, R.; Zamorano, D.; Parker, S.; Simon, D.; Lund, B.; Voit, W.; Ware, T. H. Hydrolytically Stable Thiol-Ene Networks for Flexible Bioelectronics. *ACS Appl. Mater. Interfaces* **2015**, *7*, 28673−28681.
(38) Das, A. K.; Kilty, H. P.; Marto, P. J.; Andeen, G. B.; Kumar, A. The Use of an Organic Self-Assembled Monolayer Coating to Promote Dropwise Condensation of Steam on Horizontal Tubes. *J. Heat Transfer* **2000**, *122*, 278−286.
(39) Suryanto; Haider, F. I.; Ani, M. H.; Mahmood, M. H. Modelling and Optimization of Copper Electroplating Adhesion Strength. *IOP Conf. Ser. Mater. Sci. Eng.* **2017**, *204*, 012017.
(40) Gau, W. C.; Chang, T. C.; Lin, Y. S.; Hu, J. C.; Chen, L. J.; Chang, C. Y.; Cheng, C. L. Copper Electroplating for Future Ultralarge Scale Integration Interconnection. *J. Vac. Sci. Technol., A* **2000**, *18*, 656−660.
(41) Giroire, B.; Ali Ahmad, M.; Aubert, G.; Teule-Gay, L.; Michau, D.; Watkins, J. J.; Aymonier, C.; Poulon-Quintin, A. A Comparative Study of Copper Thin Films Deposited Using Magnetron Sputtering and Supercritical Fluid Deposition Techniques. *Thin Solid Films* **2017**, *643*, 53−59.
(42) Komalakrishna, H.; Augustin, A.; Bhat, K. U. Electron Beam Deposition of Copper Thin Film on Aluminium Substrate and Its Characterization. *Am. J. Mater. Sci.* **2015**, *5*, 19−24.
(43) Schneider, C. A.; Rasband, W. S.; Eliceiri, K. W. NIH Image to ImageJ: 25 Years of Image Analysis. *Nat. Methods* **2012**, *9*, 671−675.
(44) Lau, K. K. S.; Caulfield, J. A.; Gleason, K. K. Variable Angle Spectroscopic Ellipsometry of Fluorocarbon Films from Hot Filament Chemical Vapor Deposition. *J. Vac. Sci. Technol., A* **2000**, *18*, 2404.
(45) Miljkovic, N.; Enright, R.; Wang, E. N. Effect of Droplet Morphology on Growth Dynamics and Heat Transfer during Condensation on Superhydrophobic Nanostructured Surfaces. *ACS Nano* **2012**, *6*, 1776−1785.
(46) Rykaczewski, K.; Scott, J. H. J.; Fedorov, A. G. Electron Beam Heating Effects during Environmental Scanning Electron Microscopy Imaging of Water Condensation on Superhydrophobic Surfaces. *Appl. Phys. Lett.* **2011**, *98*, 093106.

https://doi.org/10.1021/acs.langmuir.2c01477
Langmuir 2022, 38, 11296−11303